Laboratory Studies of Low-Temperature Reactions of C_2H with C_2H_2 and Implications for Atmospheric Models of Titan

Jens Olaf P. Pedersen, Brian J. Opansky, and Stephen R. Leone*,†

Joint Institute for Laboratory Astrophysics, National Institute of Standards and Technology and University of Colorado, Department of Chemistry and Biochemistry, University of Colorado, Boulder, Colorado 80309-0440

Received: January 20, 1993; In Final Form: April 13, 1993

Rate coefficients for the reaction $C_2H + C_2H_2 \rightarrow C_4H_2 + H$ are measured over the temperature range 170–350 K. The reactions are carried out in a temperature variable flow cell. C_2H radicals are produced by pulsed laser photolysis of C_2H_2, and a tunable infrared color-center laser is used to probe the transient removal of C_2H in absorption to derive the rate coefficients. The results show that the rate coefficient is independent of temperature over the range 170–350 K and equal to $(1.1 \pm 0.2) \times 10^{-10} \exp[(28 \pm 20)/T]$ cm^3 molecule^{-1} s^{-1}. The reaction studied is of central importance for models of the photochemistry of the atmospheres of the outer planets, in particular for the satellite Titan, and the implications of the present results for these models are discussed.

Introduction

The ethynyl radical, C_2H, is important in all environments containing acetylene, such as flames[1] and the atmospheres of the outer planets.[2] Ethynyl radical is known to be an important reactive intermediate in combustion processes.[3] It is also found to be among the most abundant polyatomic species observed in interstellar space,[4] and it has been inferred to exist in comets[5] and in planetary atmospheres of Jupiter,[6,7] Saturn[7] and its satellite Titan,[2,8] Uranus,[7,9,10] and Neptune[11,12] and its satellite Triton.[13] The reaction of C_2H with acetylene

$$C_2H + C_2H_2 \xrightarrow{k_{C_2H_2}} C_4H_2 + H \qquad (1)$$

is of particular importance for models[2,6-13] of the atmospheres of these outer planets and their satellites, and the product diacetylene (butadiyne), C_4H_2, is a key precursor to the formation of polyacetylene hazes and ices. Rate determinations for this reaction have, however, not been made below room temperature, and the models require an extrapolation to temperatures relevant for the outer solar system, which are 50–190 K. In this work we extend the rate data of the $C_2H + C_2H_2$ reaction to lower temperature values (170–350 K), applicable to the photochemical computer models of Titan. The satellite Titan is of particular interest because its organic chemistry has been suggested to have relevance for events leading to the origin of life on Earth.[14,15] A study of Titan is one of the major objectives of the planned Cassini Mission[16] to the Saturnian system, and the Cassini spacecraft includes a Titan atmospheric entry probe (Huygens probe).

The earliest measurements on reactions of C_2H were obtained from relative rates with various hydrocarbons.[17,18] In the work by Cullis et al.[18] a temperature-dependent rate coefficient for the reaction of C_2H with C_2H_2 was deduced, from which the value at room temperature is suggested to be 10^{-15} cm^3 molecule^{-1} s^{-1}. However, a much higher value for the room temperature rate coefficient was found in later works. Lange and Wagner[19] produced C_2H by microwave discharge in a fast-flowing bromoacetylene–helium mixture at 320 K and followed the concentration of C_2H and various products using a mass spectrometer. Because mixing with C_2H_2 was estimated to be incomplete in their observation zone, the rate coefficient of 5×10^{-11} cm^3 molecule^{-1} s^{-1} for $C_2H + C_2H_2$ was only given as a lower limit.

Laufer and Bass[20] produced C_2H by flash photolysis of C_2H_2 and studied the reaction $C_2H + C_2H_2$ by following the appearance of the product C_4H_2 using ultraviolet absorption spectroscopy. They reported a value of $(3.1 \pm 0.2) \times 10^{-11}$ cm^3 molecule^{-1} s^{-1} for the rate coefficient.

Stephens et al.[21] utilized a method, which is also used here, in which the C_2H radicals are produced by photolyzing acetylene and the C_2H concentration is probed using a tunable color center laser. Their value for the rate coefficient, $(1.5 \pm 0.1) \times 10^{-10}$ cm^3 molecule^{-1} s^{-1}, is higher than the two earlier results, and Stephens et al.[21] suggested that since they followed the disappearance of reactants and not the appearance of products, the reaction may involve an undetected intermediate, such as an isomer of C_4H_2. It is then only after slow isomerization to C_4H_2 that ultraviolet absorption is observed. Stephens et al.[21] also suggested a reaction scheme involving $C_4H_3^{\ddagger}$ as a long-lived intermediate.

Shin and Michael[22] measured the rate coefficient by monitoring H atom formation from reaction 1. They obtained data at room temperature and in the range 1226–1475 K by using a shock tube technique in which C_2H is produced by photolyzing acetylene and H atoms are detected by resonance absorption. Their room temperature measurements give a rate coefficient of $(1.3 \pm 0.3) \times 10^{-10}$ cm^3 molecule^{-1} s^{-1}, in good agreement with the result by Stephens et al.[21] thus ruling out the possibility of $C_4H_3^{\ddagger}$ as a long-lived intermediate. The average value for their high-temperature measurements is $(2.5 \pm 0.7) \times 10^{-10}$ cm^3 molecule^{-1} s^{-1}, but due to the substantial uncertainty, these authors note that a temperature variation in the rate coefficient is not certain.

The most recent room temperature rate coefficients are also confirmed in studies by Koshi et al.,[23,24] where the appearance of H atoms is detected by laser-induced fluorescence at the Lyman-α wavelength[23] and by detecting the appearance of C_4H_2 with time-resolved mass spectrometry.[24] Shock tube measurements at 1600–2177 K and measurements performed at 409 and 438 K by Koshi et al.[24] do not indicate a temperature dependence above room temperature, and a rate constant of $(1.5 \pm 0.3) \times 10^{-10}$ cm^3 molecule^{-1} s^{-1} is obtained by a simple average of their measurements. Since this result is based on following the appearance rate of C_4H_2 by mass spectroscopy, the suggestion[21] of an intermediate C_4H_2 isomer is in principle still possible.

In view of the earlier discrepancy among the data and the need for low-temperature data in the photochemical computer models of Titan, we have measured the rate coefficient for the $C_2H + C_2H_2$ reaction over the temperature range 170–350 K. The photochemical computer models can be tested by their ability to

* To whom correspondence should be addressed.
† Staff Member, Quantum Physics Division, National Institute of Standards and Technology.

0022-3654/93/2097-6822$04.00/0

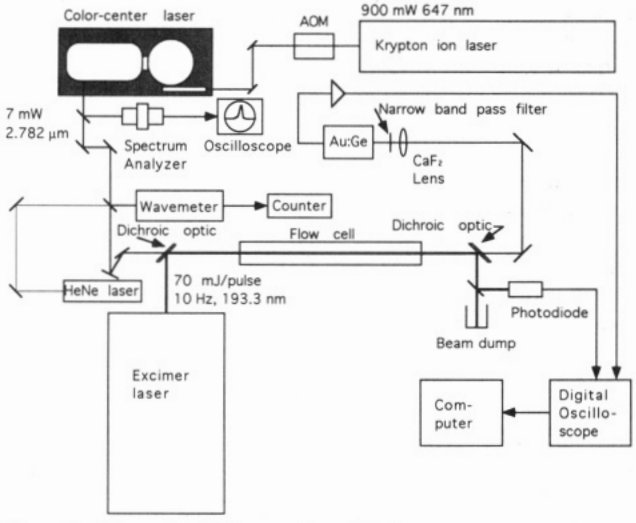

Figure 1. Schematic of the experimental setup.

reproduce the observed composition of the planetary atmospheres. Methane is the most abundant carbon species in the atmospheres of the outer planets, and photolysis of CH_4 results in production of saturated and unsaturated hydrocarbons, such as ethane and acetylene. The predictions of the photochemical computer models are very sensitive to the rate coefficient of reaction 1. In the extensive model for Titan's atmosphere by Yung et al.,[2] the rate coefficient of Laufer and Bass,[20] with a value 3.1×10^{-11} cm^3 molecule^{-1} s^{-1}, was originally used. Upon changing the value of the rate coefficient to the recent result of 1.5×10^{-10} cm^3 molecule^{-1} s^{-1}, there is an increase in the predicted ethane number density by a factor of 10, and acetylene increases by a factor of 2.[25]

Although a stable C_4H_3 was ruled out as an intermediate in reaction 1, vibrationally excited $C_4H_3^{\ddagger}$ radicals may well participate, and the reaction is thought to proceed by an addition–decomposition mechanism:[22]

$$C_2H + C_2H_2 \rightarrow [C_4H_3]^{\ddagger} \rightarrow C_4H_2 + H \qquad (2)$$

The $C_4H_3^{\ddagger}$ radical was observed in a small concentration by Lange and Wagner,[19] but the results of Shin and Michael[22] suggest that the lifetime of $C_4H_3^{\ddagger}$ with respect to unimolecular dissociation is on the order of 10^{-11} s. A pressure dependence of the reaction where the vibrationally excited $C_4H_3^{\ddagger}$ radicals are thermally stabilized is therefore not expected at modest pressures.

In this work we generate ethynyl radicals from acetylene precursors photolytically using a pulsed excimer laser, and a tunable infrared color-center laser is used to monitor the concentration of C_2H radicals in absorption. The reaction cell is surrounded by an insulated jacket through which a coolant is flowed, and this allows us to vary the temperature of the cell. Our measurements at room temperature agree well with the more recent data[21-24] and also show that the $C_2H + C_2H_2$ reaction is independent of pressure and temperature over the ranges measured in this work (170–350 K and 1.3–13.3 kPa). We further suggest that revisions of the model for Titan's atmosphere[2] are necessary.

Experimental Technique

A schematic of the experimental setup is shown in Figure 1. Briefly, ethynyl radicals are generated by photolysis of acetylene in a flow cell using a pulsed 193.3-nm excimer laser. A high-resolution, tunable infrared color-center laser at 2.78 μm probes the transient concentrations of the C_2H directly in absorption on the $A^2\Pi$–$X^2\Sigma$ transition to extract the kinetic rate coefficients.

The kinetic experiments are carried out in a temperature variable cylindrical flow cell, of length 100 cm and diameter 2.5 cm, where the photolysis and probe laser beams are overlapped over the full length of the cell. The cell is made of quartz and is constructed with a series of transverse inlets and pump-outs. This transverse arrangement allows rapid removal of the photolysis products from the probe volume. The cell is surrounded by an insulated jacket into which a coolant is flowed. Several different coolants have been used. Gaseous nitrogen was first used by flowing it through a copper coil submerged in a liquid nitrogen dewar. The temperature of the nitrogen gas and thus the reaction cell can be controlled by adjusting the nitrogen gas flow. A fluid coolant (50% ethanol and 50% methanol) was used in an improved arrangement by circulating it with a low-temperature centrifugal pump through the cell jacket and through a copper coil submerged in an ethanol–liquid nitrogen slush. The temperature of the coolant is then adjusted by the amount of liquid nitrogen added to the slush. Temperatures above room temperature are obtained by replacing the circulating ethanol/methanol coolant with water and immersing the copper coil in a water reservoir, in which the temperature is controlled by an immersion heater. The different setups allow a temperature range from 170–350 K to be covered. A type K thermocouple samples the gas temperature inside the cell, and the pressure is measured with a 100-Torr (13.3-kPa) absolute capacitance manometer. The cell windows are constructed of double Suprasil W1 optical flats with an evacuated region between them to prevent condensation on the outer window.

The photolysis laser is a rare gas halide excimer operated on argon fluoride, at a repetition rate of 5–30 Hz, typically 10 Hz, and with a pulse energy of 20–130 mJ, typically 70 mJ. The excimer beam is overlapped with the probe laser beam using a dichroic mirror having 95% reflectance at 193 nm when operated at 45° incidence. After exiting the cell, the excimer is directed into a beam dump using another dichroic mirror. These mirrors are long-wavelength pass filters, with about 90% transmission of the probe laser beam over its entire tuning range from 2.3 to 3.3 μm. The excimer beam path is continuously purged with a nitrogen flow to avoid absorption by O_2 and production of ozone.

In all experiments the C_2H concentration is monitored from the ground vibronic state, on the $Q_{22}(10)$ line of the 3600-cm^{-1} band of the $A^2\Pi$–$X^2\Sigma$ transition at 3594.393 cm^{-1}.[21,26] This transition was chosen because of its strong absorption.[21] The color center laser operates on a RbCl:Li crystal and is pumped with 900 mW of the 647-nm line from a krypton ion laser. The color-center laser typically produces an output of about 7 mW. Single-frequency operation is achieved using an intracavity etalon in the tuning arm chamber of the laser; the tuning arm chamber is evacuated and back-filled with nitrogen to avoid absorption from close-lying H_2O lines. Coarse tuning is accomplished by tuning the grating end mirror. After coarse adjustment, the etalon can be tuned and aligned piezoelectrically, and fine-tuning of the wavelength is done using a piezoelectrically driven folding mirror to change the resonator length.

In the first experiments intensity variations in the krypton ion laser were found to cause deteriorated C_2H signals. The root-mean-square (rms) noise on the ion laser beam was 2.5% and was found to be responsible for a similar noise on the probe laser beam. The noise is reduced by inserting an acousto-optic modulator into the pump beam. The modulator is driven by fast-feedback electronics and splits off most of the intensity variations above a constant amplitude, so that the transmitted pump beam has a rms noise of 1%. This causes a similar rms noise of about 1% in the probe laser beam.

The longitudinal mode structure of the color center laser is monitored with a scanning Fabry-Perot spectrum analyzer, and a traveling wave meter[27] is used for monitoring the wavelength. The Michelson interferometer wavemeter uses a frequency stabilized single-mode helium–neon laser to produce the reference fringes and has an accuracy of 0.01 cm^{-1}, which enables an easy identification of the C_2H lines. The calibration of the wave meter is checked by measuring the well-known Br($^2P_{3/2}$–$^2P_{1/2}$) lines at 2.71 μm.

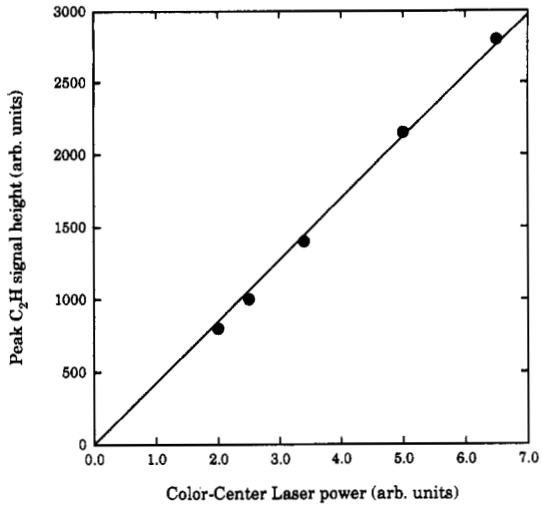

Figure 2. Plot of peak C_2H signal height vs color-center laser power.

After traversing the reaction cell, the beam from the color center laser is focused on a 50-MHz liquid N_2 cooled Ge:Au detector with a sensitive area of 20 mm^2. The high-speed transient signals corresponding to the transmitted power of the color center laser are amplified and co-added using a digital oscilloscope to improve the signal-to-noise ratio. The digital oscilloscope is interfaced with a computer in which the data are stored. For a typical measurement, transient absorption signals from 1000 excimer pulses are averaged. The data collection is started after each excimer pulse with a signal from a photodiode which is triggered by the excimer pulse. Scattered light from the windows is removed from the signals by orienting the cell windows about 10° from normal incidence of the incoming excimer beam and by using a narrow band-pass infrared filter in front of the Ge:Au detector.

The basis state carrying the oscillator strength for the transition from the ground state of acetylene at 193 nm is the $\tilde{A}\ ^1A_u\ 10\ \nu_3$ *trans*-bending level.[28] After excitation, C_2H_2 can undergo decomposition into C_2H and H. However, production of C_2H + H is not very efficient, with a quantum yield of only 0.26 ± 0.04.[29] The major product appears to be metastable acetylene, $C_2H_2^{**}$, which is believed to be $^3B_2$ vinylidene, H_2CC:.[30] The energy of the C–H bond in acetylene has been measured to be 549.3 ± 2.9 kJ mol^{-1},[31] and with the 193.3-nm photon energy of 619 kJ mol^{-1} an energy of ~69.0 kJ mol^{-1} is available for the products of the C_2H + H fragmentation. Since the $A^2\Pi$ state of C_2H is only ~47.8 kJ mol^{-1} above the $X^2\Sigma$ electronic ground state, the radicals can be both electronically and vibrationally excited. The internal excitation of the C_2H radicals has been studied by Fletcher and Leone,[32] who observed five states in emission after 193-nm photolysis, and by Balko et al.[31] and Segall et al.,[34] who studied the energy distribution of H atom fragments from the photolysis with a time-of-flight (TOF) technique. The TOF distributions[33,34] showed a fast, unstructured part, followed by a series of well-resolved peaks. Since the energy distribution mirrors the C_2H internal energy distribution, C_2H is at first highly excited and must be subsequently relaxed for the kinetics studies, as discussed below. The fast component in the TOF distributions measured by Balko et al.[33] and Segall et al.[34] were assigned to C_2H photolysis in which excited C_2 was formed. Cool and Goodwin[35] have, e.g., observed C_2 bands with intensities which had a quadratic dependence on photolysis laser energy, indicative of C_2 formation by secondary photolysis. In order to test the influence of multiphoton processes and secondary dissociation, we measured the decay constants of the C_2H signal (see section III) for a range of laser energies and repetition rates. It was found that the C_2H signal depends linearly on the color center laser power (see Figure 2), and the decay constants were invariant with the excimer repetition rate and pulse energy within the ranges used in this work (5–30 Hz and 20–130 mJ).

The photon energy is also sufficient to dissociate acetylene directly into $C_2 + H_2$, but the energy is close to the threshold for this channel, which requires 602 kJ mol^{-1},[29] and Wodtke and Lee[36] found the yield to be less than 15% of the C_2H + H channel. This places an upper limit to the quantum yield for the $C_2 + H_2$ channel of 0.05, and we can therefore neglect this contribution.

In the experiment, a mixture of acetylene, a rare gas buffer, and a vibrational relaxer is flowed through the cell. The rare gas buffer ensures translational thermalization and a rapid equilibration with the temperature of the walls of the flow cell. The efficiency of various electronic and vibrational relaxers was investigated, and sulfur hexafluoride (SF_6) was found to give good results. Tetrafluoromethane (CF_4) was less efficient but was used for the lowest-temperature studied in this work because of its higher vapor pressure. Helium was used as the rare gas buffer. All gases were obtained commercially with the following purities: He, 99.99%; SF_6, 99.98%; CF_4, 99.99%; C_2H_2, 99.6%. Since commercial acetylene contains traces of acetone, the gas is purified by flowing it through an activated charcoal filter.

The flow rate of each gas is measured using mass flow meters. All gases are mixed by injecting them into a separate mixing cell of length 25 cm and diameter 1.5 cm in a direction opposite to the outlet from the cell in order to introduce turbulence. The flow velocity through the mixing cell is about 1 m/s, and further turbulence is introduced by flowing the mixture through a 7-cm-long Pyrex tube with a number of indentations on the walls. The mixture is then passed through a coil immersed in a slush bath in order to trap impurities before flowing into the main reaction cell. The mass flow meters are calibrated for each gas by flowing the gas into a cylinder with a well-determined volume and measuring the pressure rise as a function of time.

Partial pressures for each gas are calculated from the measured flow rates and total pressure. Measurements are taken for different acetylene densities (0.5–10) × 10^{15} cm^{-3}, for total pressures between 1.3 and 13.3 kPa (10–100 Torr), and for temperatures between 170 and 350 K. The rate coefficients of reaction 1 are then derived from measurements of the transient removal of the C_2H concentration at varying densities of the acetylene precursor gas. The absorption cross section of C_2H_2 at 193.3 nm is 1.35 × 10^{-19} cm^2,[29] and with a quantum yield of 0.26 for production of C_2H,[29] this results in a C_2H concentration of 5 × 10^{13} cm^{-3} for the highest acetylene density. The acetylene density thus remains nearly constant, and the reaction follows pseudo-first-order kinetics. With typical total flow rates of 1.5 × 10^{20} molecules s^{-1}, the volume photolyzed by the excimer is completely replaced every 0.5 s (typically every five excimer pulses).

A rapid deposition of photolysis products was initially observed on the inside of the cell windows. An inlet to each end of the cell was added so that the windows could be cleaned after each series of measurements, preventing a major buildup of photolysis deposits.

Another problem is the formation of a thermal lens[37] in the gas after photolysis and thermal heating. Careful alignment of the laser beams, clean excimer optics, and restricting the maximum pulse energy to about 70 mJ reduced the effects of thermal lensing significantly.

Results and Discussion

From reaction 1 the following kinetic relation is applicable:

$$d[C_2H(t)]/dt = -k_{C_2H_2}[C_2H(t)][C_2H_2(t)] \qquad (3)$$

where $k_{C_2H_2}$ is the bimolecular rate coefficient. Since all experiments were performed under pseudo-first-order conditions

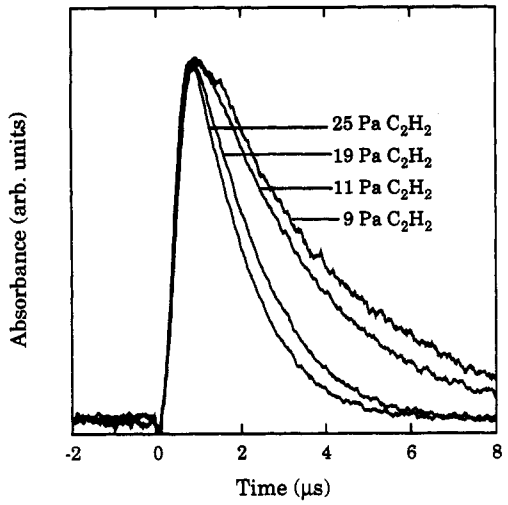

Figure 3. Typical C_2H absorption traces versus time for a total pressure of 4 kPa and for C_2H_2 partial pressures between 9 and 25 Pa. All traces have been normalized to the 9-Pa trace.

with $[C_2H_2] \gg [C_2H]$ by a factor of 200–1000, $[C_2H_2]$ is essentially constant. After integration of eq 3

$$[C_2H(t)] = [C_2H]_0 \exp(-k_{obs}t) \quad (4)$$

the observed rate coefficient k_{obs} is related to the bimolecular rate constant $k_{C_2H_2}$ by the following

$$k_{obs} = k_{C_2H_2}[C_2H_2] \quad (5)$$

The C_2H concentration can be determined from the fractional absorption of the probe laser beam via Beer's law

$$I(t) = I_0 e^{-\sigma n(t) l} \quad (6)$$

where I is the transmitted power of the infrared beam, σ is the cross section for absorption of the infrared radiation by C_2H, $n(t)$ is the number density for C_2H radicals in the ground vibrational state, and l is the absorption path length, which is equal to the cell length since the excimer beam and the smaller infrared beam are collinear.

The cross section σ is not known, but we show below that $\sigma n(t)l$ is very small (weak absorption), and we can therefore rewrite (6) as

$$I(t) = I_0(1 - \sigma n(t)l) \quad (7)$$

The concentration of C_2H radicals in the ground vibrational state is then given as

$$n(t) = (I_0 - I(t))/\sigma l I_0 \quad (8)$$

and is thus proportional to the relative change in transmission of the infrared beam. Since the transmitted power is proportional to the voltage output V from the detector, we have

$$n(t) = (V_0 - V(t))/\sigma l V_0 \quad (9)$$

Figure 3 shows typical results for $V_0 - V(t)$ for different acetylene concentrations, with each trace having been normalized to the 9-Pa C_2H_2 trace to show the change in time constant with various acetylene pressures. The zero on the time axis is determined by the trigger signal from the excimer beam. The signals are seen to rise from zero to a maximum value in about 0.9 μs and then decay over several microseconds. Since the photolysis flash duration is ≈20 ns and the detector rise time is 20 ns, this indicates that almost all of the C_2H radicals, as expected, are created in excited states in the photolysis of acetylene whereafter they decay to the ground state, and this causes the initial rise of the signal. As the population of excited radicals is depleted and the ground-state radicals undergo reaction, the signal eventually decays.

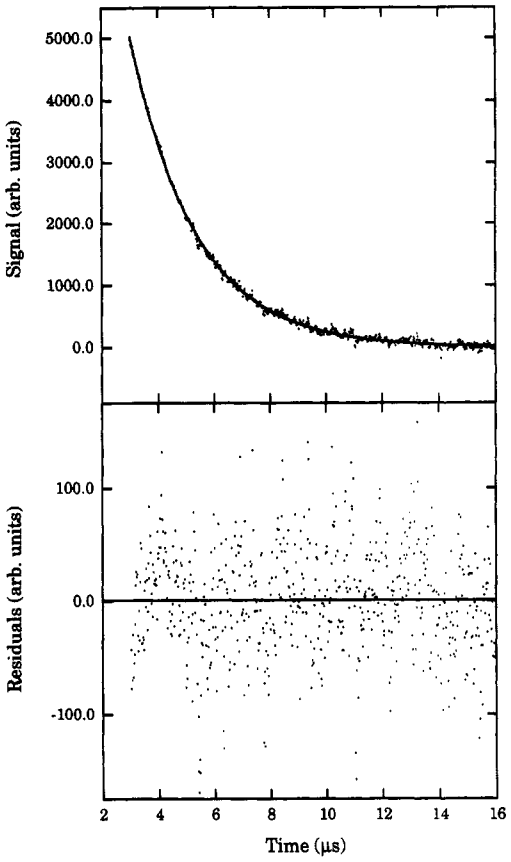

Figure 4. (a) C_2H decay due to reaction with C_2H_2. The solid line is the fitted single-exponential decay. (b) The residuals to the fit.

Reaction of excited C_2H radicals does not influence our measurement of the rate coefficient with C_2H in the X(0,0,0) state, because we directly observe the rate of removal of ground-state radicals. We do, however, require a rapid thermalization of the radicals and therefore use a large excess of buffer gas and an additional vibrational relaxer. In addition to being quenched by the buffer gas, there is a base deactivation by C_2H_2 on C_2H. With no additional vibrational relaxer added, the signal rise time is 1.8 μs. For a total pressure of 4 kPa and a ratio of about 5 between the concentration of the vibrational relaxer, SF_6, and the C_2H_2 concentration, the signal rise time t_1 was found to be 1.2 μs. This rise time decreased to 0.9 μs for a ratio between these concentrations of 25. Typically, a ratio of 100 between the SF_6:C_2H_2 concentrations was used, but no further decrease in t_1 was observed for higher ratios at the same total pressure. With CF_4 as the vibrational relaxer we found $t_1 \approx 1.5$ μs for a total pressure of 4 kPa and a ratio of 100 between the CF_4:C_2H_2 concentrations. The fast initial rise of the signal is nonexponential, but we estimate a time constant for the rise time and then assume that after a factor of 3 longer than this time constant the decay of the signal is dominated by the reactions of ground-state C_2H radicals. In this part of the recorded signal we can now relate $V_0 - V(t) \propto n(t) = [C_2H(t)]$ given by eq 4 and determine k_{obs} by fitting the signal to eq 4 with a nonlinear least-squares program. We neglect contributions from radical–radical reactions and reactions with product molecules and recombination, since the average radical–radical collision time is ≈100 μs. Diffusion out of the probe volume to the walls at the typical pressure of 4 kPa occurs over several milliseconds and also contributes negligibly to the decay. Figure 4 shows an example of a fit of eq 4 to the data and the corresponding residuals.

We measured the quantity $V_0 - V(t_1)$, where t_1 is again the signal rise time, as a function of the power of the infrared beam,

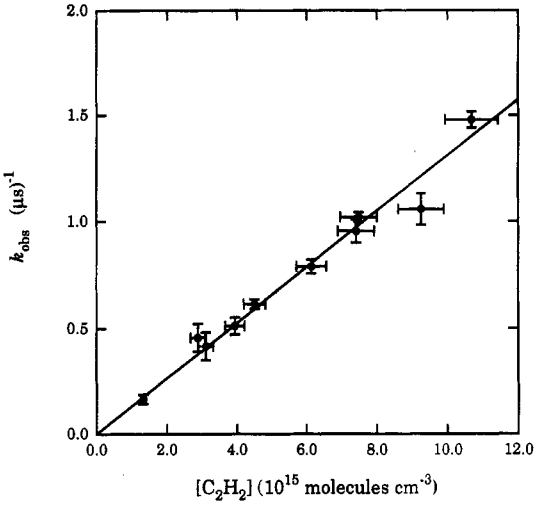

Figure 5. Plot of observed decay coefficient k_{obs} vs C_2H_2 concentration. These data were taken at 300 K, and $k_{C_2H_2}$ for this particular plot is (1.3 ± 0.2) × 10^{-10} cm^3 molecule^{-1} s^{-1}.

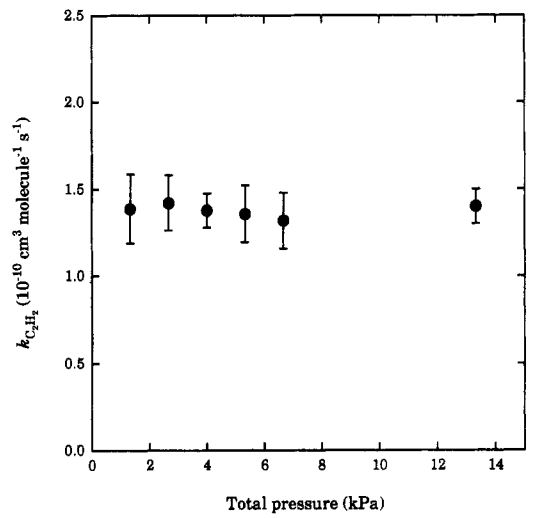

Figure 6. Rate coefficient $k_{C_2H_2}$ for the reaction $C_2H + C_2H_2$ at room temperature and for total pressures between 1.3 and 13 kPa.

which is proportional to V_0. As was mentioned before, the quantity $V_0 - V(t_1)$ was found to have a linear dependence on V_0; see Figure 2. This supports the assumption above that we can use the limit of weak absorption in Beer's law.

The observed decay coefficient k_{obs} is related to the bimolecular rate coefficient $k_{C_2H_2}$ by eq 5. Figure 5 shows a plot of k_{obs} vs $[C_2H_2]$ at 300 K, and the value of $k_{C_2H_2}$ is then determined by a linear least-squares fit. The uncertainty in the acetylene concentration is calculated from the accumulated uncertainties in the instruments used to obtain the pressure, temperature, and flow rate measurements. This uncertainty together with the uncertainty in k_{obs} is then used to calculate the resulting uncertainty on $k_{C_2H_2}$. Typically, this leads to a relative error on $k_{C_2H_2}$ of ±12%.

The rate coefficients $k_{C_2H_2}$ as a function of pressure at room temperature are shown in Figure 6. No pressure dependence is apparent in the investigated range of 1.3–13.3 kPa, and the room temperature rate coefficient can therefore be given as $k_{C_2H_2}$(298 K) = (1.3 ± 0.2) × 10^{-10} cm^3 molecule^{-1} s^{-1}. This is consistent with the data of Shin and Michael,[22] where the rate at room temperature was measured for pressures between 3.3 and 12.7 kPa, also without showing any pressure dependence, and reported to be $k_{C_2H_2}$(298 K) = (1.3 ± 0.3) × 10^{-10} cm^3 molecule^{-1} s^{-1}. Our value for the room temperature rate coefficient also agrees well with the other recent determinations of Stephens et al.[21] and

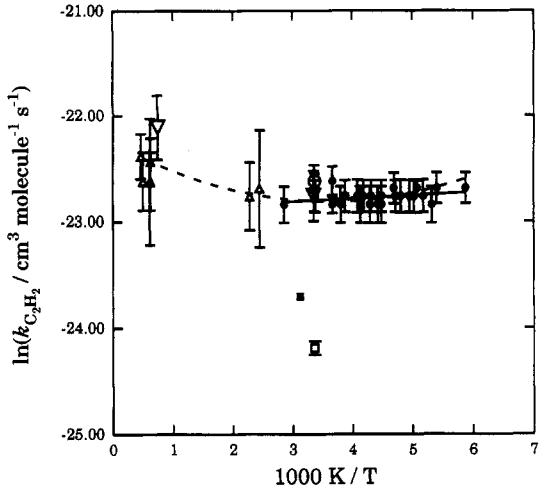

Figure 7. Experimental data for $C_2H + C_2H_2 \rightarrow C_4H_2 + H$: ●, this work; ■, Lange and Wagner;[19] □, Laufer and Bass;[20] ○, Stephens et al.;[21] ▽, Shin and Michael;[22] △, Koshi et al.[23,24] The solid line is the fit to this work $k_{C_2H_2} = A \exp(-E_a/RT)$, and the dotted line is the fit to this work, the work of Shin and Michael, and the work of Koshi et al. to $k_{C_2H_2} = AT^{1/2} \exp(-E_a/RT)$.

Koshi et al.,[23,24] who studied the reaction at a total pressure of 0.7 kPa.

The temperature dependence of the rate coefficients is shown in Figure 7. Here the natural logarithm of $k_{C_2H_2}$ is shown as a function of the inverse temperature, for a constant total gas density of 5 × 10^{17} cm^{-3} for our data. This plot shows that a simple Arrhenius fit (solid line) is equal to (1.1 ± 0.2) × 10^{-10} exp[(28 ± 20)/T] cm^3 molecule^{-1} s^{-1} with an E_a = −0.2 ± 0.2 kJ mol^{-1}. The results of previous determinations by other groups[19–24] have also been included in Figure 7. The average value for the high-temperature (1226–1475 K) results by Shin and Michael[22] is (2.5 ± 0.7) × 10^{-10} cm^3 molecule^{-1} s^{-1}, and these authors note that this may indicate a slight temperature dependence above room temperature, but because of their experimental uncertainties this was not a definite conclusion. The five high-temperature (1600–2177 K) measurements of Koshi et al.[24] show less scatter, and a simple average gives the value (1.6 ± 0.3) × 10^{-10} cm^3 molecule^{-1} s^{-1}. Since Koshi et al.[24] also measured $k_{C_2H_2}$ at 409 and 439 K and found a rate coefficient of (1.4 ± 0.3) × 10^{-10} and (1.3 ± 0.3) × 10^{-10} cm^3 molecule^{-1} s^{-1}, respectively, they concluded that the rate coefficient was constant over the temperature range 298–2177 K. Our results at 350 K and below further confirm this conclusion. The data from the present work and the work of Stephens et al.,[21] Shin and Michael,[22] and Koshi et al.[23,24] can also be fit by the complete Arrhenius expression (dotted line) $AT^{1/2} \exp(-E_a/RT)$, which is equal to 4.1 × $10^{-12}T^{1/2}$ exp[(173 ± 12)/T] and gives an E_a = −1.4 ± 0.1 kJ mol^{-1}.

It should be noted that, within the error bars of all the experimental results, no definite temperature dependence has been observed. The energy of activation calculated based on fits to different Arrhenius expressions indicates that there is little or no barrier to formation of $C_4H_3^‡$ or unimolecular decomposition to products.

Since the rate coefficients based on C_2H depletion (ref 19 and this work) are in agreement with those based on H atom and C_4H_2 formation,[22–24] an earlier suggestion[21] that $C_4H_3^‡$ could be a long-lived intermediate in the reaction has been ruled out. The magnitude of $k_{C_2H_2}$ and the lack of a temperature dependence over 170–2177 K are consistent with an addition mechanism followed by reaction in the association limit. The lack of a pressure dependence, as indicated in Figure 6, suggests that the addition complex, $C_4H_3^‡$, has an extremely short lifetime. Shin and Michael have estimated that the lifetime with respect to unimolecular dissociation to products is ~10^{-11} s. Thus, the

$C_4H_3^‡$ complex cannot dissociate back to $C_2H + C_2H_2$ or undergo collisional stabilization to C_4H_3.

A kinetic scheme for the reaction is as follows:

$$C_2H + C_2H_2 \underset{k_{-1}+k'_{-1}[M]}{\overset{k_1}{\rightleftharpoons}} C_4H_3^‡ \xrightarrow{k_3+k'_3[M]} C_4H_2 + H \quad (10)$$

$$C_4H_3^‡ \xrightarrow{k_2[M]} C_4H_3$$

where we allow for both spontaneous and collision-induced removal of $[C_4H_3^‡]$. The rate of disappearance of C_2H can be expressed as

$$d[C_2H]/dt = -k_1[C_2H][C_2H_2] - k_{-1}[C_4H_3^‡] + k'_{-1}[C_4H_3^‡][M] \quad (11)$$

Likewise, the rate of disappearance of $C_4H_3^‡$ is

$$d[C_4H_3^‡]/dt = k_1[C_2H][C_2H_2] - k_{-1}[C_4H_3^‡] - k'_{-1}[C_4H_3^‡][M] - k_2[C_4H_3^‡][M] - k_3[C_4H_3^‡] - k'_3[C_4H_3^‡][M] \quad (12)$$

Applying the steady-state approximation to $[C_4H_3^‡]$ and solving for $[C_4H_3^‡]$, we find that

$$[C_4H_3^‡] = \frac{k_1[C_2H][C_2H_2]}{k_{-1} + k'_{-1}[M] + k_2[M] + k_3 + k'_3[M]} \quad (13)$$

The rate of disappearance for C_2H can be rewritten after eq 13 has been substituted into eq 11

$$\frac{d[C_2H]}{dt} = -k_1[C_2H][C_2H_2] \times \left(1 - \frac{k_{-1} + k'_{-1}[M]}{k_{-1} + k'_{-1}[M] + k_2[M] + k_3 + k'_3[M]}\right) \quad (14)$$

where $k_{obs} = k_1k_{eff}[C_2H_2] = k_{C_2H_2}[C_2H_2]$ and k_{eff}, the "effective" rate of removal of $C_4H_3^‡$, is

$$k_{eff} = 1 - \frac{k_{-1} + k'_{-1}[M]}{k_{-1} + k'_{-1}[M] + k_2[M] + k_3 + k'_3[M]} \quad (15)$$

After integration of eq 14 and the appropriate substitutions

$$[C_2H]_t = [C_2H]_0 \exp(-k_1[C_2H_2]k_{eff}t) \quad (16)$$

On the basis of kinetic results, we are most likely operating in the region where collisional effects can be neglected, where $k_{eff} = 1 - k_{-1}/(k_{-1} + k_3)$. The number densities in this experiment range from 3.2×10^{17} to 3.2×10^{18} cm^{-3}, and no pressure dependence is observed. The complex would have to live for $\sim 10^{-9}$ s in order to experience a collision. Although no RRK or RRKM calculations have been done on $C_4H_3^‡$, comparison with the isoelectronic CN radical may be helpful. The rates of CN reaction with C_2H_2 have been studied recently by several authors[38-40] in the temperature range 175–740 K, and extensions of the range to lower temperatures (80 K) are in progress.[41] The reaction is assumed[38-40] to proceed via a similar addition–elimination mechanism:

$$CN + C_2H_2 \rightarrow NCC_2H_2^‡ \rightarrow C_2HCN + H \quad (17)$$

The reaction has been found to be independent of total pressure, and the rate shows only a small (negative) temperature dependence. The room temperature rate coefficient is about 2.5×10^{-10} cm^3 $molecule^{-1}$ s^{-1}, which is very similar to the result for $C_2H + C_2H_2$. The exothermicity of reaction 17 is also similar,

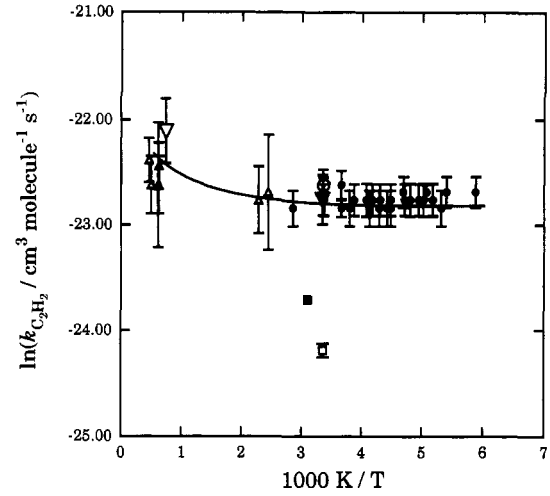

Figure 8. Lennard-Jones corrected collisional rate constant curve is calculated from eq 15 using a steric factor of 0.25. Symbols are the same as in Figure 7.

about 87 kJ mol^{-1}. RRKM calculations[39] for the activated $NCC_2H_2^‡$ give a lifetime of 10^{-11} s, and therefore the lifetime of $C_4H_3^‡$ may be comparable. Therefore, in eq 15 k_3 is much larger than either $k_2[M]$, $k'_{-1}[M]$, or $k'_3[M]$.

Consequently, the major channels that remove $C_4H_3^‡$ are spontaneous back-dissociation to reactants or unimolecular dissociation to products. As noted above, the small or zero temperature dependence of the rate coefficient suggests that there is little or no activation barrier for formation of the $C_4H_3^‡$ complex. Depending on the values of the heats of formation for C_4H_3 and C_2H used,[3,36] the $C_4H_3^‡$ complex is formed with 297–317 kJ mol^{-1} of energy. Reaction 1 is exothermic by 92–122 kJ mol^{-1}, and the energy of the unimolecular dissociation process is therefore $\approx$205 kJ mol^{-1} above ground state of C_4H_3, whereas the energy of the back-dissociation process is at the threshold energy. Given the large exothermicity to form products, phase-space arguments suggest that $k_3 \gg k_{-1}$; therefore, $k_{eff} \sim 1$. This reduces the experimental observations to eq 4, with $k_{obs} = k_1[C_2H_2]$.

The $C_2H + C_2H_2$ reaction can also be discussed in terms of collision theory. The measured rate is found to be of the same order as the hard-sphere collisional values. A more accurate model is the Lennard-Jones corrected collisional rate constant[42]

$$Z_{12} = \sigma_{12}^2\Omega(2,2)^*(8\pi kT/\mu)^{1/2} \quad (18)$$

where k is Boltzmann's constant, T is the temperature, μ is the reduced mass of the colliding molecules, and σ_{12} is the collision diameter. The quantities $\Omega(2,2)^*$ are tabulated collision integrals which are functions of $T^* = kT/\epsilon_{12}$, where ϵ_{12} is the intermolecular potential well depth for the interacting species. The collision integrals are precisely the factor by which the rate constant differs from the hard-sphere rate. We can use the geometric mean approximation to estimate $\epsilon_{12} = (\epsilon_1\epsilon_2)^{1/2}$, where ϵ_1/k and ϵ_2/k are the force constants for C_2H_2 and C_2H, respectively, and similarly we estimate $\sigma_{12} = (\sigma_1+\sigma_2)/2$. If we use the Lennard-Jones parameters for C_2H_2 given by Hirschfelder et al.[43] for both C_2H_2 and C_2H, we can calculate the theoretical curve shown in Figure 8, which has been scaled as discussed below. Shin and Michael[22] have suggested that a steric factor of 0.5 should be used to account for orientation effects. This value can be justified because in the addition reaction of the linear C_2H radical to the acetylene molecule one can assume that the radical is only favorably aligned in 50% of the collisions. The Lennard-Jones rate overestimates the experimental data, but the good agreement shown in Figure 8 is obtained by using a steric factor of 0.25. This may be an indication that the alignment of the linear C_2H_2 molecule is also important for the addition process. The simple model also indicates that the only rate-determining step in the addition–

elimination reaction of C_2H with C_2H_2 is the formation of the addition complex.

Implications for Atmospheric Models of Titan

The hydrocarbon-rich atmospheres of the outer planets have been modeled both in laboratory experiments[13,44,45] and in photochemical computer calculations.[6-12] In the experimental investigations the atmospheric chemistry induced by magnetospheric electrons or other charged particles is simulated using a cold plasma discharge excited in a continuously flowing gas mixture approximating the planet's stratospheric composition.[46,47] The production efficiencies of the molecules produced in the experiment are derived, and using a simple atmospheric mixing model and calculated rates for the flux of charged particles, predictions can be made for the atmospheric abundance of hydrocarbons and nitriles. In the photochemical computer models a predicted composition is also derived from a few parent molecules using a comprehensive set of chemical reactions. Both approaches have been applied specifically to the atmosphere of Titan, Saturn's large satellite. Since the laboratory simulations do not include photochemical input, they will underestimate the abundance of molecules which are primary photochemical products. In spite of this, the computed abundance of molecules from laboratory simulations have been found to be in better agreement with recent data for Titan derived from Voyager IRIS (infrared interferometer spectrometer) spectra[48,49] than photochemical computer modeling. In particular, the mean abundances of several hydrocarbons and most of the nitriles estimated from observation are much lower than those given by the Yung et al. model.[2] The photochemical models, however, give a better insight into the processes which produce hydrocarbon species in Titan's atmosphere, and with minor modifications, the same basic scheme of reactions and rate coefficients can be used to gain an approximate understanding of the atmospheres of all of the outer planets and many of their satellites. Aside from the need to include charged particle-induced chemistry explicitly, a major uncertainty in such models continues to be the limited availability of appropriate kinetics data.[50] The present work is part of a project to provide some of the relevant data. The $C_2H + C_2H_2$ reaction has been identified[25] as one of the key reactions in the models, motivating this initial study.

Titan is the only satellite in the solar system with a substantial atmosphere. Since the surface temperature is only 94 K and the surface pressure is 50% higher than the Earth's,[16] the density of the atmosphere at the surface is much higher than on Earth. Images taken by Voyager 1 showed that Titan is completely covered by a thick orange haze which masks the surface. It is thought that the organic chemistry in Titan's atmosphere may resemble that of the Earth's primitive atmosphere before life began. Titan is therefore of high scientific interest.

The existence of an atmosphere on Titan was first suggested in 1908 by Solá,[51] and methane was discovered in Titan's atmosphere in 1944 by Kuiper[52] from near-infrared spectra. The most current and accurate information on Titan's atmosphere was obtained during Voyager 1 and 2 Saturn flyby missions in 1980 and 1981. The atmosphere is now known to be composed mainly of molecular nitrogen (75–99%) and methane (0.5–3.4%). The presence of argon (0–27%) has been suggested on a cosmological basis,[8,53] but has not been observed directly, and the specific mole fractions of the major species have therefore not been well-defined. A number of small molecules have also been observed and their mole fractions measured directly. The most abundant are hydrogen (0.2–0.6%), carbon monoxide (60 ppm), ethane (10 ppm), acetylene (2 ppm), and propane (0.5 ppm).[54]

Methane is believed to be the ultimate precursor for more complex hydrocarbons in the atmosphere. Compared to the atmospheres of Jupiter and Saturn, where atmospheric methane is also present, the abundances of complex hydrocarbons in Titan's atmosphere are greater. Molecular and atomic hydrogen both escape from Titan's atmosphere due to Titan's weak gravitational acceleration and "warm" thermosphere (~186 K), leaving behind complex hydrocarbons and nitriles to accumulate in Titan's atmosphere[8] and sediment to its surface. Recent work has shown that these organic sediments will be subject to impact-mediated aqueous alteration, allowing nitriles and unsaturated hydrocarbons to produce several classes of prebiochemically significant molecules there.[14,15]

One of the challenges to models has been to explain the high abundance of ethane on Titan. Ethane appears to be the main product of CH_4 photochemistry, and once it is formed it is fairly stable.[2] Since the branching ratio into $CH_4 + h\nu \rightarrow CH_3 + H$ is considered unimportant,[2,55] formation of ethane cannot be explained by direct photolysis of CH_4 into $CH_3 + H$ followed by recombination of two CH_3 radicals. Recent photodissociation studies by Ashfold et al.[56] indicate that this assumption may be incorrect. However, photodissociation of CH_4 (which requires light of wavelength shorter than about 145 nm) does occur in the high atmosphere[2,54] where the pressure is too low to enhance the recombination process by a third body. Other principal products from CH_4 photolysis are $^1CH_2 + H_2$ and $CH_2 + 2H$, where $^1CH_2$ and CH_2 are the excited (singlet) and ground (triplet) state, respectively.[2] Reactions of $^1CH_2$ with H_2 can produce CH_3 radicals and thus account for the ethane observed on Jupiter and Saturn, where H_2 is abundant. On Titan, however, the large amount of N_2 in the atmosphere will quench 95% of the $^1CH_2$ radicals produced[2] before reaction and thus lead to a much lower ethane production. Other schemes which will lead to production of ethane have therefore been proposed.

Already before the Voyager observations, Allen et al.[57] proposed that photolysis of acetylene, which only requires wavelengths shorter than 200 nm, could lead to additional dissociation of CH_4 on Titan:

$$C_2H_2 + h\nu \rightarrow C_2H + H \quad (19)$$

$$C_2H + CH_4 \rightarrow C_2H_2 + CH_3 \quad (20)$$

$$\text{net:} \quad CH_4 \rightarrow CH_3 + H \quad (21)$$

Another precursor to CH_3 is diacetylene, C_4H_2, which can also be produced in Titan's atmosphere by the photolysis of acetylene:

$$C_2H_2 + h\nu \rightarrow C_2H + H \quad (18)$$

$$C_2H + C_2H_2 \rightarrow C_4H_2 + H \quad (1)$$

$$\text{net:} \quad 2C_2H_2 \rightarrow C_4H_2 + 2H \quad (22)$$

The production of diacetylene in Titan's atmosphere is important because it is a precursor for formation of complex hydrocarbons.[58] In addition, since diacetylene can also be discussed by light of wavelength shorter than 200 nm, it acts as a catalyst for collecting solar energy used to break apart CH_4,[57] producing

$$C_4H_2 + h\nu \rightarrow 2C_2H \quad (23)$$

$$C_2H + CH_4 \rightarrow C_2H_2 + CH_3 \quad (20)$$

$$C_2H + C_2H_2 \rightarrow C_4H_2 + H \quad (1)$$

$$\text{net:} \quad CH_4 \rightarrow CH_3 + H \quad (21)$$

The above schemes yield a photocatalytic dissociation of CH_4

and provide the CH_3 radicals necessary for the formation of ethane:

$$CH_3 + CH_3 + M\ (M = N_2, CH_4, ...) \rightarrow C_2H_6 + M \quad (24)$$

It was mentioned in the Introduction that the Yung et al.[2] model is rather sensitive to the $C_2H + C_2H_2$ reaction and that changing the rate coefficient for this reaction from the value of 3.1×10^{-11} cm^3 molecule^{-1} s^{-1} originally used to 1.5×10^{-10} cm^3 molecule^{-1} s^{-1} increases the ethane number density by a factor of 10 and the acetylene density by a factor of 2.[25] Since the model produces values for the acetylene concentration that already overestimate the IRIS data as found by Coustenis et al.[48] by a factor of 20 and the ethane concentration is overestimated by a factor of 8, the present results indicate the need for further revisions of other rate coefficients used in the model. In addition, some changes to the model itself may be necessary.

One reason for the discrepancy may be an incorrect estimate of the eddy diffusion coefficient. Steiner and Bauer[59] recently derived an eddy diffusion coefficient in the altitude range 150–600 km, where some of the organic synthesis occurs, which is about an order of magnitude smaller than the value utilized by Yung et al.[2] The large predicted abundances of complex hydrocarbons are also the consequence of very low model concentrations of H atoms, which could otherwise suppress the formation of higher hydrocarbons by reactions that break multiple bonds. Nava et al.[60] have found that the $C_4H_2 + H$ reaction, which catalyzes H atom recombination to molecular hydrogen, has a rate coefficient at Titan's temperatures about 10 times smaller than the value used by Yung et al.[2]

In summary, we have studied the $C_2H + C_2H_2$ reaction and found the rate coefficient for the reaction to be independent of temperature for $T = 170$–350 K. The low-temperature data are relevant in understanding the abundances of numerous hydrocarbons that make up Titan's complex atmosphere and in discerning the relative importance of photochemical versus charged-particle sources for the organic gases and solids found there. Accurate results from this study will improve the photochemical computer models of Titan's atmosphere. As can be seen from the reaction schemes above, the rate coefficients for the $C_2H + CH_4$ reaction 17 are also of importance for the models, and measurements of this reaction at low temperatures are in progress.

Acknowledgment. We gratefully acknowledge the National Aeronautics and Space Administration for support of this research. J.O.P.P. also thanks the Danish Natural Science Research Council for support. We would also like to thank Paul W. Seakins for his helpful discussions.

References and Notes

(1) Kern, R. D.; Xie, K. *Prog. Energy Combust. Sci.* **1991**, *17*, 191.
(2) Yung, Y. L.; Allen, M.; Pinto, J. P. *Astrophys. J. Suppl. Ser.* **1984**, *55*, 465.
(3) Kiefer, J. H.; Von Drasek, W. A. *Int. J. Chem. Kinet.* **1990**, *22*, 747.
(4) Tucker, K. D.; Kutner, M. L.; Thaddeus, P. *Astrophys. J.* **1974**, *193*, L115.
(5) Jackson, W. M.; Bao, Y.; Urdahl, R. S. *J. Geophys. Res.* **1991**, *96*, 17569.
(6) West, R. A.; Strobel, D. F.; Tomasko, M. G. *Icarus* **1986**, *65*, 161.
(7) Atreya, S. K.; Romani, P. N. *Recent Advances in Planetary Meteorology*; Hunt, G. E., Ed.; Cambridge University Press: New York, 1985; p 17.
(8) Strobel, D. F. *Planet. Space Sci.* **1982**, *30*, 839.
(9) Pollack, J. B.; Rogers, K.; Pope, S. K.; Tomasko, M. G.; Romani, P. N.; Atreya, S. K. *J. Geophys. Res.* **1987**, *92*, 15037.
(10) Summers, M. E.; Strobel, D. F. *Astrophys. J.* **1989**, *346*, 495.
(11) Romani, P. N.; Atreya, S. K. *Icarus* **1988**, *74*, 442.
(12) Moses, J. I.; Allen, M.; Yung, Y. L. *Icarus* **1992**, *99*, 318.
(13) Thompson, W. R.; Singh, S. K.; Khare, B. N.; Sagan, C. *Geophys. Res. Lett.* **1989**, *16*, 981.
(14) Raulin, F.; Frère, C.; Do, L.; Khlifi, M.; Paillous, P.; Vanssay, E. de. *Proc. Symp. Titan*, Toulouse, France, 9–12 Sept 1991, *ESA SP*-338.
(15) Thompson, W. R.; Sagan, C. *Proc. Symp. Titan*, Toulouse, France, 9–12 Sept 1991, *ESA SP-338*.
(16) Lebreton, J.-P.; Scoon, G. *ESA Bulletin* **1988**, no. 55, 24.
(17) Tarr, A. M.; Strausz, O. P.; Gunning, H. E. *Trans. Faraday Soc.* **1965**, *61*, 1946.
(18) Cullis, C. F.; Hucknall, D. J.; Shepherd, J. V. *Proc. R. Soc. London* **1973**, *A335*, 525.
(19) Lange, W.; Wagner, H. G. *Ber. Bunsen.-Ges. Phys. Chem.* **1975**, *79*, 165.
(20) Laufer, A. H.; Bass, A. M. *J. Phys. Chem.* **1979**, *83*, 310.
(21) Stephens, J. W.; Hall, J. L.; Solka, H.; Yan, W.-B.; Curl, R. F.; Glass, G. P. *J. Phys. Chem.* **1987**, *91*, 5740.
(22) Shin, K. S.; Michael, J. V. *J. Phys. Chem.* **1991**, *95*, 5864.
(23) Koshi, M.; Nishida, N.; Matsui, H. *J. Phys. Chem.* **1992**, *96*, 5875.
(24) Koshi, M.; Fukuda, K.; Kamiya, K.; Matsui, H. *J. Phys. Chem.* **1992**, *96*, 9839.
(25) Allen, M. Private communication, 1990.
(26) Yan, W.-B.; Dane, C. B.; Zeitz, D.; Hall, J. L.; Curl, R. F. *J. Mol. Spectrosc.* **1987**, *123*, 486.
(27) Hall, J. L.; Lee, S. A. *Appl. Phys. Lett.* **1976**, *29*, 367.
(28) Foo, P. D.; Innes, K. K. *Chem. Phys. Lett.* **1973**, *22*, 439.
(29) Satyapal, S.; Bersohn, R. *J. Phys. Chem.* **1991**, *95*, 8004.
(30) Fahr, A.; Laufer, A. H. *J. Photochem.* **1986**, *34*, 261.
(31) Ervin, K. M.; Gronert, S.; Barlow, S. E.; Gilles, M. K.; Harrison, A. G.; Bierbaum, V. M.; DePuy, C. M.; Lineberger, W. C.; Ellision, G. B. *J. Am. Chem. Soc.* **1990**, *112*, 5750.
(32) Fletcher, T. R.; Leone, S. R. *J. Chem. Phys.* **1989**, *90*, 871.
(33) Balko, B. A.; Zhang, J.; Lee, Y. T. *J. Chem. Phys.* **1991**, *94*, 7958.
(34) Segall, J.; Wen, Y.; Lavi, R.; Singer, R.; Wittig, C. *J. Phys. Chem.* **1991**, *95*, 8078.
(35) Cool, T. A.; Goodwin, P. M. *J. Chem. Phys.* **1991**, *94*, 6978.
(36) Wodtke, A. M.; Lee, Y. T. *J. Phys. Chem.* **1985**, *89*, 4744.
(37) Hess, W. P.; Kohler, S. J.; Haugen, H. K.; Leone, S. R. *J. Chem. Phys.* **1984**, *84*, 2143.
(38) Lichtin, D. A.; Lin, M. C. *Chem. Phys.* **1986**, *104*, 325.
(39) Yang, D. L.; Ya, T.; Wang, N. S.; Lin, M. C. *Chem. Phys.* **1992**, *160*, 317.
(40) Herbert, L.; Smith, I. W. M.; Spencer-Smith, R. D. *Int. J. Chem. Kinet.* **1992**, *24*, 791.
(41) Herbert, L.; Li, K.; Sharkey, P.; Smith, I. W. M.; Defrance, A.; Karthauser, J.; Queffelec, J. L.; Rebrion, C.; Rowe, B. R.; Sims, I. R. In *Abstracts, 12th International Symposium on Gas Kinetics*; University of Reading: 1992; p H19.
(42) Lee, J. H.; Michael, J. V.; Payne, W. A.; Stief, L. J. *J. Chem. Phys.* **1978**, *69*, 3069.
(43) Hirschfelder, J. O.; Curtiss, C. F.; Bird, R. B. *Molecular Theory of Gases and Liquids*; Wiley: New York, 1964.
(44) Thompson, W. R.; Henry, T. J.; Schwarts, J. M.; Khare, B. N.; Sagan, C. *Icarus* **1991**, *90*, 57.
(45) Sagan, C.; Thompson, W. R.; Khare, B. N. *Acc. Chem. Res.* **1992**, *25*, 286.
(46) McDonald, G. D.; Thompson, W. R.; Sagan, C. *Icarus* **1992**, *99*, 131.
(47) Thompson, W. R.; Henry, T.; Khare, B. N.; Flynn, L.; Schwartz, J.; Sagan, C. *J. Geophys. Res.* **1987**, *92*, 15092.
(48) Coustenis, A.; Bézard, B.; Gautier, D. *Icarus* **1989**, *80*, 54.
(49) Coustenis, A. *Vis. Astron.* **1991**, *34*, 11.
(50) Yung, Y. L. *Icarus* **1987**, *72*, 468.
(51) Solá, J. C. *Astron. Nach.* **1908**, *179*, 289.
(52) Kuiper, G. P. *Appl. J.* **1944**, *100*, 378.
(53) Owen, T. *Planet. Space Sci.* **1982**, *30*, 833.
(54) Slanger, T. G.; Black, G. *J. Chem. Phys.* **1982**, *77*, 2432.
(55) Ashfold, N. M. R.; Lambert, I. R.; Mordaunt, D. H.; Morley, G. P.; Western, C. M. In *Abstracts, 12th International Symposium on Gas Kinetics*; University of Reading: 1992; p C1.
(56) Sagan, C.; Thompson, W. R. *Icarus* **1984**, *59*, 133.
(57) Allen, M.; Pinto, J. P.; Yung, Y. L. *Astron. Astrophys.* **1980**, *242*, L125.
(58) Bandy, R. E.; Lakshiminaragan, C.; Frost, R. K.; Zwier, T. S. *Science* **1992**, *258*, 1630.
(59) Steiner, G.; Bauer, S. J. *Ann. Geophys.* **1990**, *8*, 473.
(60) Nava, D. F.; Mitchell, M. B.; Stief, L. J. *J. Geophys. Res.* **1986**, *91*, 4585.